



## Reaction mechanism and thermoelectric properties of $\text{In}_{0.22}\text{Co}_4\text{Sb}_{12}$ prepared by magnesiothermy

Sylvain Le Tonquesse, Eric Alleno, Valérie Demange, Carmelo Prestipino,  
Olivier Rouleau, Mathieu Pasturel

### ► To cite this version:

Sylvain Le Tonquesse, Eric Alleno, Valérie Demange, Carmelo Prestipino, Olivier Rouleau, et al..  
Reaction mechanism and thermoelectric properties of  $\text{In}_{0.22}\text{Co}_4\text{Sb}_{12}$  prepared by magnesiothermy.  
Materials Today Chemistry, 2020, 16, pp.100223. 10.1016/j.mtchem.2019.100223 . hal-03048178

**HAL Id: hal-03048178**

**<https://univ-rennes.hal.science/hal-03048178>**

Submitted on 9 Dec 2020

**HAL** is a multi-disciplinary open access archive for the deposit and dissemination of scientific research documents, whether they are published or not. The documents may come from teaching and research institutions in France or abroad, or from public or private research centers.

L'archive ouverte pluridisciplinaire **HAL**, est destinée au dépôt et à la diffusion de documents scientifiques de niveau recherche, publiés ou non, émanant des établissements d'enseignement et de recherche français ou étrangers, des laboratoires publics ou privés.

# Reaction mechanism and thermoelectric properties of $\text{In}_{0.22}\text{Co}_4\text{Sb}_{12}$ prepared by magnesiothermy

Sylvain Le Tonquesse<sup>a</sup>, Éric Alleno<sup>b</sup>, Valérie Demange<sup>a</sup>, Carmelo Prestipino<sup>a</sup>,  
Olivier Rouleau<sup>b</sup>, Mathieu Pasturel<sup>a</sup>,

<sup>a</sup>Univ Rennes, CNRS, Institut des Sciences Chimiques de Rennes - UMR6226, F-35000, Rennes, France

<sup>b</sup>Université Paris-Est, Institut de Chimie et des Matériaux Paris-Est, UMR 7182 CNRS - UPEC, 2 rue H. Dunant, 94320 THIAIS, France

---

## Abstract

The magnesiothermy synthesis of  $\text{In}_{0.22}\text{Co}_4\text{Sb}_{12}$  with high In-rattler concentration from  $\text{Sb}_2\text{O}_3$  and In-doped  $\text{Co}_3\text{O}_4$  precursors is reported. This process directly yields a submicronic powder in a single step of 96 h at 810 K. The reaction mechanism has been investigated by stopping the reaction every 12 h and quantifying the existing phases by X-ray diffraction and Rietveld refinements. The precursors are first reduced in  $\text{CoO}$  and  $\text{Sb}_2\text{O}_3$  lower oxides, then form  $\text{CoSb}_2\text{O}_6$  and  $\text{CoSb}_2\text{O}_4$  intermediates which are finally reduced in  $\text{In}_x\text{Co}_4\text{Sb}_{12}$ . A powder with 350 nm average size and mostly composed of In-filled skutterudite phase with composition close to  $\text{In}_{0.17}\text{Co}_4\text{Sb}_{12}$  is obtained. Upon spark plasma sintering, small residual amount of  $\text{InSb}$  reacts with the skutterudite matrix to form a single-phase densified pellet with composition close to  $\text{In}_{0.22}\text{Co}_4\text{Sb}_{12}$ . The resulting densified material with 1.8  $\mu\text{m}$  average grain size shows a figure-of-merit  $ZT_{\text{max}}$  of 0.95 at 750 K.

**Keywords:** Skutterudites; Magnesiothermy synthesis; Reaction mechanism; Thermoelectric properties.

---

---

\*mathieu.pasturel@univ-rennes1.fr; Institut des Sciences Chimiques de Rennes, Campus de Beaulieu, bat. 10A, 263 avenue Général Leclerc, 35042 Rennes Cedex, France

# 1. Introduction

Thermoelectric (TE) materials enable the direct conversion of heat into electricity through the Seebeck effect. The conversion efficiency is directly related to the figure-of-merit  $ZT$  defined as:

$$ZT = \frac{\alpha^2}{\rho (\kappa_L + \kappa_e)} T \quad (1)$$

with  $\alpha$  the Seebeck coefficient,  $\rho$  the electrical resistivity,  $\kappa_L$  and  $\kappa_e$  the lattice and electronic contributions to the total thermal conductivity  $\kappa$  and  $T$  the temperature. CoSb<sub>3</sub>-based skutterudites are well-known TE materials with a band gap of about 0.2 eV [1]. They are considered as promising candidates for mid-temperature (600 - 800 K) TE applications because of their excellent electronic properties, good mechanical properties and relatively abundant constituting elements. Large power factors,  $PF = \alpha^2/\rho$ , reaching 4 - 5 mW m<sup>-1</sup> K<sup>-2</sup> can be obtained for compositions with optimized charge carrier concentration. In order to achieve high  $ZT$ , the intrinsic high thermal conductivity ( $\approx 9$  W m<sup>-1</sup> K<sup>-1</sup> at 298 K for CoSb<sub>3</sub> [2]) must be reduced as much as possible without simultaneously degrading the electronic properties. This can be effectively done by partially filling the empty isocahedral voids of the structure with rare-earth, alkaline metal or III - IV group elements [1]. The additional mass contrast induced by the partial occupancy as well as the ‘rattling’ behavior of the filling atoms in the oversized voids effectively scatter acoustic heat-carrying phonons. For example, lattice thermal conductivities as low as 1 - 2 and  $\approx 0.5$  W m<sup>-1</sup> K<sup>-1</sup> were reported for single Ba-, Ca- and Yb-filled [3, 4, 5] and nanostructured multi-filled skutterudites [6], respectively.

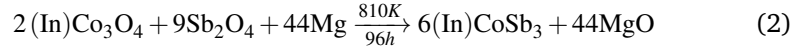
Indium is among the most studied filler atom for  $n$ -type skutterudites because (i) it acts as an electron donor enabling large increase of  $PF$  and (ii) it

efficiently reduces  $\kappa_L$  due to its heavy atomic mass. While some controversy exists about its true solubility limit ( $0.16 < x < 0.27$ ) [7, 8, 9], all authors agree that the best performances are obtained by maximizing the In concentration [2, 10].  $ZT_{max}$  of about 1.1 are usually reported for materials with composition close to  $\text{In}_{0.25}\text{Co}_4\text{Sb}_{12}$  and synthesized by conventional fusion/solidification processes [11, 2]. However, due to the peritectic formation of  $\text{CoSb}_3$ , long annealing ( $> 100$  h) at high temperature (1100 K) are required to form a single phase product. In addition, the ingots are composed of microns sized grains which need to be reduced by milling in order to reduce  $\kappa_L$ .  $\kappa$  reduction were attempted using such conventional approach by *in situ* formation of InSb nano-precipitates [12, 13, 14] or by designing mesostructured materials with oxide nanoinclusions [11, 15]. These additional annealing and milling steps, to be performed under unreactive atmosphere, cost time and energy cost and could become an obstacle to the large scale production of this material.

Alternative processes have been developed to overcome the problematic synthesis of this material. For example, hydrothermal [16, 17] or melt-spinning/reactive spark plasma sintering approaches [18] have been adapted to the synthesis of nanostructured  $\text{In}_x\text{Co}_4\text{Sb}_{12}$  with high concentration of interfaces between the grains and lattice thermal conductivity as low as  $1.5 \text{ W m}^{-1} \text{ K}^{-1}$ . Most importantly, these alternative routes do not require any post-reaction annealing which considerably speed up the synthesis. However, nanostructured materials often suffer from largely higher electrical resistivity usually attributed to the lower density of the sintered materials [19, 16] or to the enhanced charge carriers scattering at the numerous interfaces/defects, considerably reducing the beneficial effect of the microstructure on  $ZT$ .

In a previous article [20], we reported a new magnesio-reduction synthesis

52 for  $\text{In}_x\text{Co}_4\text{Sb}_{12}$  with  $x = 0.13$  according to the reaction:



53 This process, also applied to the production of TE-silicides [21], possesses  
54 many advantages such as the direct synthesis of high purity skutterudite pow-  
55 ders with submicronic average grain sizes without additional long annealing or  
56 milling step, high yield, relatively low reaction temperature and the use of cheap  
57 and air-stable oxide precursors. Moreover, magnesiothermy is already used to  
58 industrially produce metals via the Kroll [22] or Ames [23] processes and of-  
59 fer thus interesting scalability perspectives. In the present article, this magne-  
60 sioreduction process is adapted to the synthesis of saturated  $\text{In}_{0.22}\text{Co}_4\text{Sb}_{12}$ . The  
61 discussion will mainly focus on the comprehension of the reaction mechanism  
62 which was investigated by X-ray diffraction (XRD). Finally, the thermoelectric  
63 properties were measured and compared to those of reference samples from the  
64 literature.

## 65 2. Experimental procedures

66 The detailed procedure for the magnesiothermy synthesis of In-filled skut-  
67 terudites according to reaction (2) is described in a previous work [20]. For  
68 preparation of the ' $\text{In}_{0.18}\text{Co}_{2.81}\text{O}_4$ ' precursor, stoichiometric amounts of  $\text{CoCl}_2 \cdot 6\text{H}_2\text{O}$   
69 (Prolabo, 99.9 %) and  $\text{In}(\text{NO}_3)_3 \cdot x\text{H}_2\text{O}$  (home-made by dissolving In in concen-  
70 trated  $\text{HNO}_3$ ) are dissolved in distilled water and then precipitated using NaOH.  
71 The precipitate is washed with water and ethanol several times, dried at 363 K  
72 and calcined at 723 K for 4 h in air. XRD pattern (fig. SI 1) shows broad diffrac-  
73 tion peaks corresponding to  $\text{Co}_3\text{O}_4$  and  $\text{In}_2\text{O}_3$ . Rietveld refinement converges to  
74 a lattice parameter  $a = 8.137(9)$  Å significantly larger than for pristine  $\text{Co}_3\text{O}_4$   
75 ( $a = 8.076$  Å [24]) suggesting the insertion of In in the structure [25]. The pres-

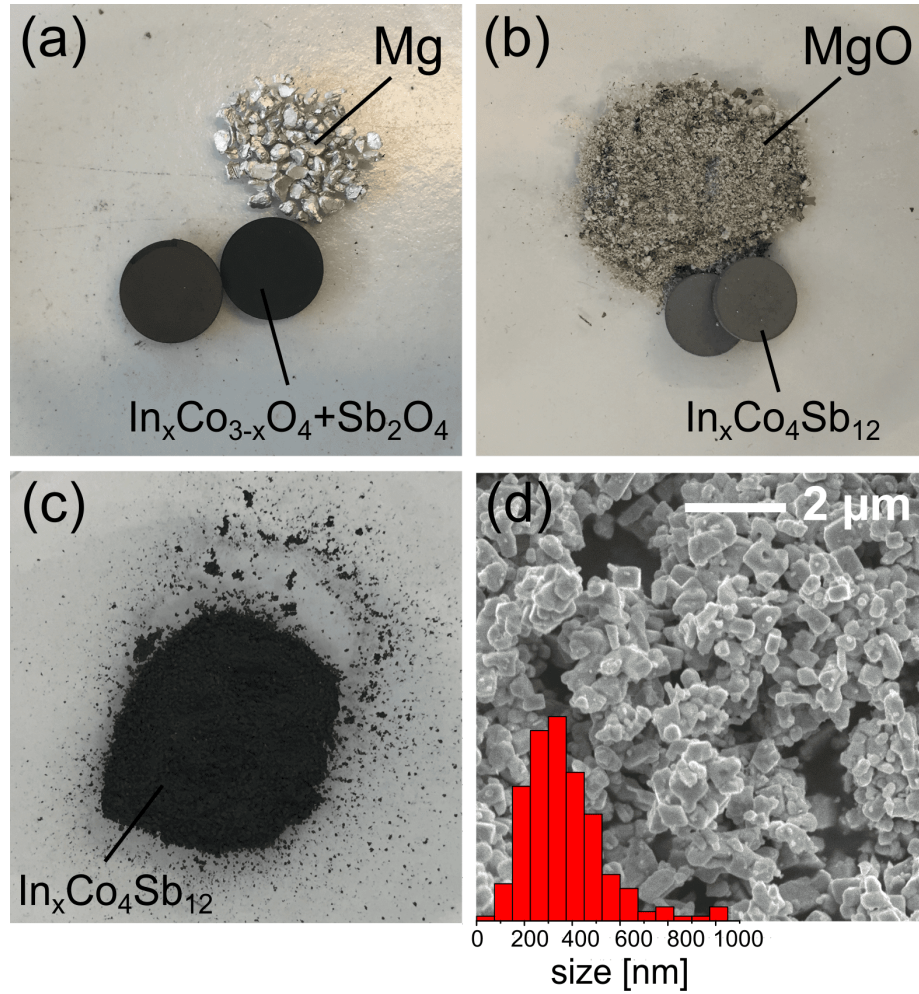


Figure 1: Pictures of (a) the reaction precursors, (b) reaction products after 96 h at 810 K and (c) crushed as-synthesized  $\text{In}_x\text{Co}_4\text{Sb}_{12}$  pellets. (d) Secondary electron SEM image of the as-synthesized powder with histogram showing the grain size distribution.

ence of remaining  $\text{In}_2\text{O}_3$  indicates that the solubility limit has been reached. A mixture of this precursor and  $\text{Sb}_2\text{O}_4$  (Sigma-Aldrich, 99.995 %) with 1:5.4 molar composition, required to counterbalance the loss of antimony by evaporation during the MR process and obtain phase pure samples [20], is thoroughly milled in an agate mortar. The oxide mixture is cold-pressed at 250 MPa into  $\varnothing$  10 mm pellets with about 2 mm height (fig. 1a). The pellets (usually 2 stacked on top

of each other) are placed with Mg chunks (2 - 3 % excess) in a clamped Mo crucible. The crucible is heated to 810 K for 96 h under protective Ar atmosphere before being cooled down to room temperature. After the reaction, the skutterudite remains in the shape of compact pellets and can easily be separated from the loose MgO (fig. 1b). The powder (fig. 1c,d) is then spark plasma sintered (FCT HP-D-10 system) in Ø 10 mm graphite dies at 1000 K and 66 MPa for 10 min.

Powder X-ray diffraction was performed on a Bruker D8 Advance diffractometer in the  $\theta$ - $2\theta$  Bragg-Brentano geometry working with a monochromatized Cu  $K\alpha_1$  radiation ( $\lambda = 1.5406 \text{ \AA}$ ), equipped with a LynxEye detector which enables photon energy discrimination around 20 %, thus reducing the cobalt fluorescence signal. Lattice parameters and phase fractions were determined by the Rietveld method using the FullProf software [26]. Scanning electron microscopy (SEM) images and energy dispersive spectroscopy (EDS) were performed on a JEOL JSM 7100 F microscope equipped with an Oxford EDS SDD X-Max spectrometer. Transport properties measurements were carried out using a home-made apparatus described elsewhere [27]. Thermal diffusivity measurements were performed using a Netzsch LFA 457 equipment under Ar atmosphere. The thermal conductivity was determined from  $\kappa = D C_p d$  with  $D$  the thermal diffusivity,  $C_p$  the specific heat of the sample calculated using the Dulong-Petit law and  $d$  the sample density determined by the Archimede method in absolute ethanol.

### 3. Results and discussion

#### 3.1. Reaction mechanism and skutterudite characterizations

$\text{In}_x\text{Co}_4\text{Sb}_{12}$  (targeted  $x = 0.25$ ) has been synthesized, along with some InSb and Sb impurities, from  $\text{Sb}_2\text{O}_3$  and In-doped  $\text{Co}_3\text{O}_4$  after 96 h heat treatment

at 810 K in presence of Mg. To elucidate the reaction mechanism, the synthesis was repeated several times and stopped every twelve hours. Each time, the phases in the samples were quantified by the Rietveld method and their relative concentrations are represented in fig. 2. Figure 3 shows some selected XRD patterns while all refined patterns and parameters can be found in supplementary information (fig. SI 2, tables SI. 1 - 9). Up to 6 different phases have been identified in some patterns indicating a complex reaction mechanism. The full reduction of the precursors is realized in three steps: (i) the partial reduction of the precursors in lower oxides (0 h - 24 h), (ii) the formation of  $\text{CoSb}_2\text{O}_6$  and  $\text{CoSb}_2\text{O}_4$  intermediates (0 h - 48 h) and (iii) the complete reduction of the intermediates and the formation of  $\text{In}_x\text{Co}_4\text{Sb}_{12}$  (38 h - 96 h).

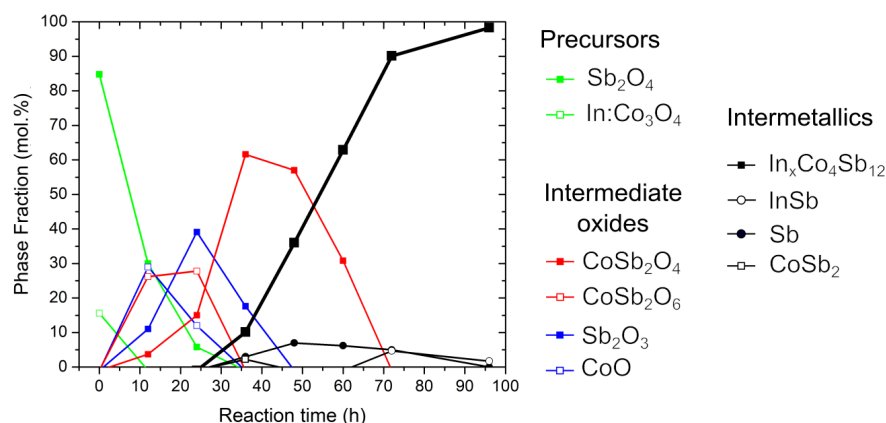


Figure 2: Evolution of the sample composition during the magnesiorreduction synthesis of  $\text{In}_x\text{Co}_4\text{Sb}_{12}$ , determined by the Rietveld method, as a function of the reaction time. In the present case and according to [28], the relative standard deviation on the concentrations are considered to be well below 5 %.

The precursors mixture is initially composed of  $\text{Sb}_2\text{O}_4$  [ $\text{Sb}^{3+}$ ,  $\text{Sb}^{5+}$ ] and  $\text{In:Co}_3\text{O}_4$  [ $\text{Co}^{2+}$ ,  $\text{Co}^{3+}$ ]. After 24 h at 813 K,  $\text{In:Co}_3\text{O}_4$  and  $\text{Sb}_2\text{O}_4$  almost completely disappeared. Instead, freshly formed  $\text{CoO}$  [ $\text{Co}^{2+}$ ] and  $\text{Sb}_2\text{O}_3$  [ $\text{Sb}^{3+}$ ] represent almost 50 % of the reaction media. This suggests the partial reduction of



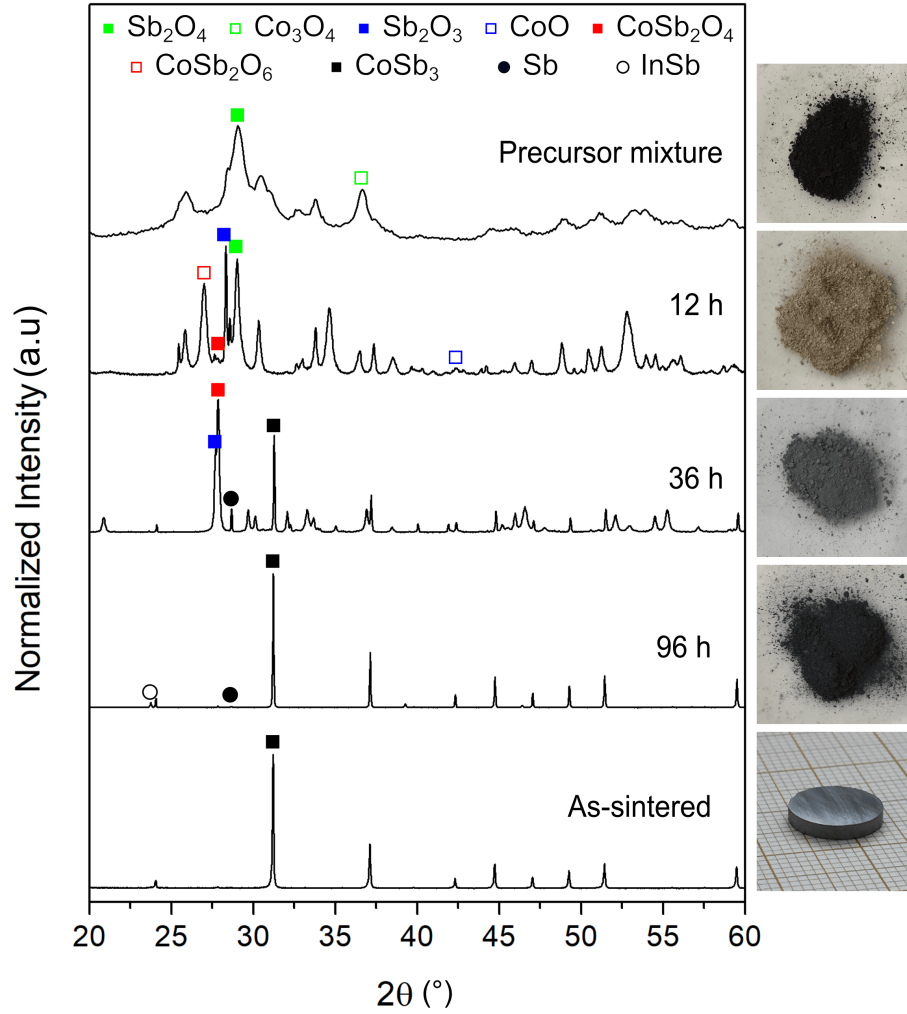


Figure 3: XRD patterns of the  $\text{In}_x\text{Co}_4\text{Sb}_{12}$  magnesioreduction synthesis after 0 h, 12 h, 36 h, 96 h reaction time and after spark plasma sintering. The symbols indicate the most intense reflections of each constituting phases. The images shows the evolution of the product color with the reaction time.

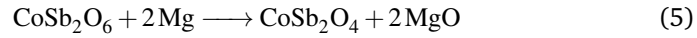
123 the precursors in lower oxides by Mg according to the reactions:





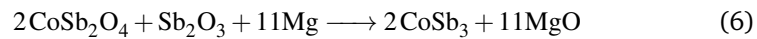
124 These reductions are thermodynamically possible at 810 K as indicated by  
 125 the large negative Gibbs free energy of reaction. In addition,  $\text{CoSb}_2\text{O}_6$  [ $\text{Co}^{2+}$ ,  
 126  $\text{Sb}^{5+}$ ] ( $P4_2/mnm$ ) and  $\text{CoSb}_2\text{O}_4$  [ $\text{Co}^{2+}$ ,  $\text{Sb}^{3+}$ ] ( $P4_2/mbc$ ) ternary intermediates  
 127 are formed most likely by solid state reactions between the various binary ox-  
 128 ides in presence. This is supported by several works reporting the synthesis of  
 129 these mixed oxides by conventional solid-state reaction starting from  $\text{CoO}$  and  
 130  $\text{Sb}_2\text{O}_3/\text{Sb}_2\text{O}_5$  powders between 973 and 1073 K [30, 31, 32].

131 After 36 h, no trace of  $\text{CoSb}_2\text{O}_6$  remains in the XRD pattern (fig. 3) and  
 132  $\text{CoSb}_2\text{O}_4$  is the major phase representing 60 mol.% of the sample. According to  
 133 the simultaneous decrease of  $\text{CoSb}_2\text{O}_6$  and increase of  $\text{CoSb}_2\text{O}_4$  contents, one  
 134 might expect  $\text{CoSb}_2\text{O}_4$  to be formed from the reduction of  $\text{CoSb}_2\text{O}_6$  according  
 135 to:

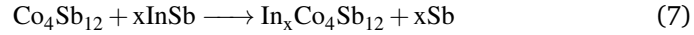


136 More interestingly, skutterudite starts forming ( $\approx 10 \%$ ) and the lattice pa-  
 137 rameter  $a = 9.0384(8) \text{ \AA}$  corresponds well to  $\text{In}_x\text{Co}_4\text{Sb}_{12}$  with low In-content  
 138 ( $x < 0.05$ ) [7, 8]. At this point of the reaction,  $\text{Sb}^{5+}$  and  $\text{Co}^{3+}$  are no more  
 139 present in the reaction media and  $\text{Sb}^{3+}$  and  $\text{Co}^{2+}$  are consecutively reduced in  
 140 metallic Co and Sb.

141 The complete reduction of  $\text{CoSb}_2\text{O}_4$  and  $\text{Sb}_2\text{O}_3$  into  $\text{CoSb}_3$  takes another 36  
 142 hours according to:



Traces of InSb appear on the diffraction patterns after 72 h. We hypothesize that In was solubilized in  $\text{CoSb}_2\text{O}_4$  because (i) the formation of InSb corresponds to the total reduction of  $\text{CoSb}_2\text{O}_4$ , (ii) the refined lattice parameters of the latter,  $a = 8.5078(5) \text{ \AA}$  and  $c = 5.9316(5) \text{ \AA}$ , are significantly larger than literature data,  $a = 8.49285(7) \text{ \AA}$  and  $c = 5.92449(5) \text{ \AA}$  [30] and (iii) other elements such as  $\text{Pb}^{2+}$  can substitute Sb to a great extent in  $\text{CoSb}_2\text{O}_4$  [30]. In presence of InSb, the lattice parameter of  $\text{In}_x\text{CoSb}_3$  increases from  $9.0384(2) \text{ \AA}$  after 48 h to  $9.04872(4) \text{ \AA}$  after 96 h. This can be explained by the insertion of In in the  $\text{CoSb}_3$  structure according to:



The slow diffusion of In in  $\text{CoSb}_3$  was already stressed out by Grytsiv *et al.* [8]. After 96 h, the reaction media is mostly composed of  $\text{In}_x\text{Co}_4\text{Sb}_{12}$  with  $a = 9.04872(4) \text{ \AA}$  which corresponds to  $x = 0.17 - 0.18$  [7, 8] and of a small amount of InSb ( $\approx 4 \text{ mol.}\%$ ) and Sb ( $\approx 2 \text{ mol.}\%$ ). No traces of MgO or Mg containing compound are visible at any time on the diffraction patterns. For this reason, we hypothesize that the reduction reactions occur *via* the slow oxidation of the Mg chunks by the equilibrium  $\text{O}_2$  vapor pressure of the oxides. This is consistent with the general aspect of the Mg chunks between 24 h to 48 h which are clearly oxidized at the surface (powdery and white) but remain metallic and relatively shiny in the core.

The as-synthesized powder was spark plasma sintered to obtain pellets with 97 % relative density. The XRD pattern of the as-sintered pellet (fig. 3) is fully indexed with the skutterudite structure type. Rietveld refinement results in a lattice parameter  $a = 9.0527(2) \text{ \AA}$  which is significantly larger than that of the as-synthesized powder. Along with the disappearance of the InSb secondary phase, whose melting point (789 K) is lower than the sintering temperature, this

168 suggests that InSb reacts with the skutterudite matrix during the sintering step  
 169 thus increasing the inserted In content. According to literature data, this lattice  
 170 parameter corresponds to a true  $\text{In}_x\text{Co}_4\text{Sb}_{12}$  composition close to  $x = 0.20 - 0.22$   
 171 [7, 8]. The scenario is very similar to the synthesis of  $\text{In}_{0.13}\text{Co}_4\text{Sb}_{12}$  where about  
 172 20 % of In was inserted in the structure during the sintering step [20].

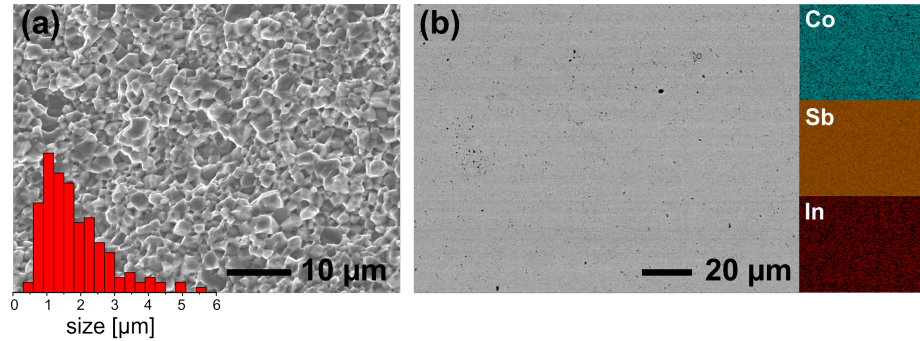


Figure 4: (a) Secondary electron SEM image of a broken cross-section of a densified  $\text{In}_{0.22}\text{Co}_4\text{Sb}_{12}$  pellet and histogram showing the distribution of the apparent grain size. (b) Backscattered electron SEM image and corresponding EDS elementary mappings of the pellet polished surface.

173 Backscattered electron image and EDS mapping of the pellet (fig. 4b) reveal  
 174 homogeneous chemical composition. Indium filling fraction could however not  
 175 be accurately quantified by EDS because of its low concentration and the partial  
 176 overlapping of the In  $L_\alpha$  and the intense Sb  $L_\alpha$  peaks. The magnesioreduc-  
 177 tion synthesis of  $\text{In}_{0.30}\text{Co}_4\text{Sb}_{12}$  was also attempted but InSb in excess leaked out  
 178 of the die during sintering and the resulting skutterudite lattice parameter re-  
 179 maind close to  $a = 9.053 \text{ \AA}$ . As a result,  $\text{In}_{0.22}\text{Co}_4\text{Sb}_{12}$  would be the In-richest  
 180 composition accessible by magnesioreduction synthesis in these reaction condi-  
 181 tions. It is in agreement with the solubility limit usually reported for In-filled  
 182  $\text{CoSb}_3$  prepared by conventional melting/annealing [8] or solid state diffusion  
 183 [33] syntheses. The SEM secondary electron image of the broken cross-section  
 184 of a pellet is shown in fig. 4a. The microstructure is typical for magnesiore-  
 185 duced skutterudite with well-faceted grains and size distribution characterized

by an average value of 1.8  $\mu\text{m}$ . The present grain size is significantly larger than our previous work [20]. This is mostly attributed to the 90 K higher sintering temperature found necessary to complete the reaction. Also the higher content of liquid InSb might have favored grain growth by accelerating matter transport during the sintering [34].

### 3.2. Thermoelectric properties

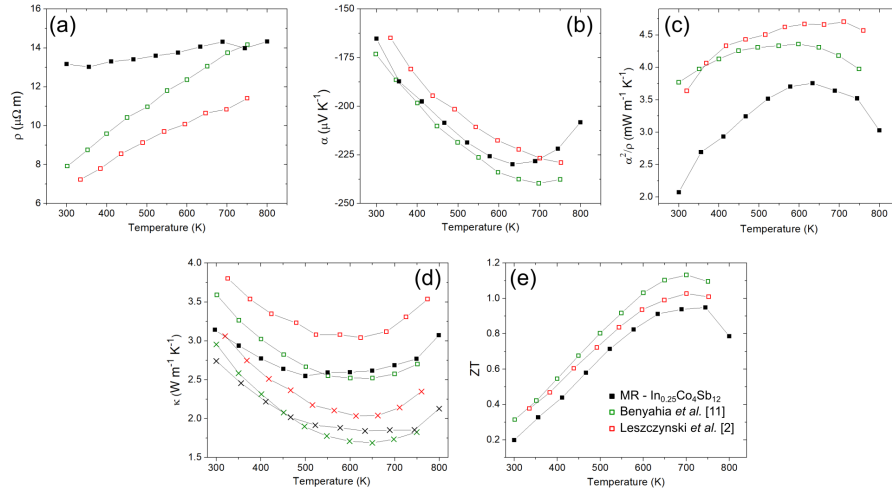


Figure 5: High-temperature dependence of (a) the electrical resistivity, (b) Seebeck coefficient, (c) power factor, (d) total (squares) and lattice (crosses) thermal conductivities and (e) figure-of-merit of  $\text{In}_{0.22}\text{Co}_4\text{Sb}_{12}$  synthesized by magnesio-reduction (filled black squares) along with literature data for  $\text{In}_{0.25}\text{Co}_4\text{Sb}_{12}$  taken from [11] (green empty squares) and  $\text{In}_{0.28}\text{Co}_4\text{Sb}_{12}$  taken from [2] (red empty squares).

The thermoelectric properties of  $\text{In}_{0.22}\text{Co}_4\text{Sb}_{12}$  are shown in fig. 5 and compared to data from the literature on compounds with similar compositions. Data reported by Benyahia *et al.* [11] and Leszczynski *et al.* [2] were obtained for materials synthesized by melting/annealing/sintering method. Although the Seebeck coefficient of our sample compares well to literature data, the resistivity is more elevated, especially near room temperature. As a direct consequence, the  $PF_{\text{max}}$  is 7 to 20 % lower at 750 K. Despite its apparent purity and density, small cracks appeared on our sample upon thermal cycles that could explain

the higher measured resistivity. Such deterioration is attributed to the melting around 800 K [8] during the measurement cycle of small residual amount of InSb usually observed at the grain boundaries of saturated In-filled skutterudite [12, 35]. However, the In content in the structure remains constant as indicated by the similar lattice parameter,  $a = 9.0520(3) \text{ \AA}$ , determined after the thermoelectric characterization.

The room temperature thermal conductivity of MR sample is about  $3.2 \text{ W m}^{-1} \text{ K}^{-1}$  and reaches its minimum value of  $2.6 \text{ W m}^{-1} \text{ K}^{-1}$  in the 450 - 650 K range. The simultaneous decrease of  $\alpha$  and upturn of  $\kappa$  at about 650 K is attributed to the bipolar effect *i.e.* to the contribution of two types of charge carriers to the material transport properties. The lattice thermal conductivity was determined by subtracting  $\kappa_e$  to  $\kappa$  and  $\kappa_e$  was calculated using the the Wiedemann-Franz law  $\kappa_e = L T/\rho$  with  $L$  taken from [2] as  $1.7 \cdot 10^{-8} \text{ W } \Omega \text{ K}^{-2}$ . The  $\kappa_L$  of the magnesiosynthesized sample agrees with the lower  $\kappa_L$  values of the literature over the entire temperature range. No significant decrease of  $\kappa_L$  is measured at room temperature contrary to our previous work on  $\text{In}_{0.13}\text{Co}_4\text{Sb}_{12}$  certainly because of the larger average grain size,  $1.8 \text{ }\mu\text{m}$  vs.  $600 \text{ nm}$ , respectively, and the stronger influence of the rattlers over the mesostructure at such elevated concentration. As a consequence of the lower  $PF$ , a  $ZT_{max}$  of 0.95 at 750 K is obtained which remains 5 and 15 % lower than the reference samples made by conventional melting/annealing process.

Further comparison of the MR-materials performance with literature data is not a straightforward task as long as the TE properties of In-filled skutterudites strongly depends on the precise In-content inserted in the cages up to its solubility limit [9, 33, 13, 36]. In the present case, we confirm that increasing the In-content from 0.13 [20] to 0.22 in the MR-samples decreases the thermal conductivity and increases the  $ZT_{max}$  from 0.75 to 0.95. Oversaturating In in

227 CoSb<sub>3</sub> induces the formation of InSb and/or CoSb<sub>2</sub> (nano)precipitates that are  
 228 playing a significant role in decreasing the thermal conductivity and improving  
 229 the  $ZT_{max}$  of these composite materials [37, 38, 39, 40]. MR-In<sub>0.22</sub>Co<sub>4</sub>Sb<sub>12</sub> do  
 230 not show the presence of such precipitates after spark plasma sintering. The  
 231 measured TE properties can thus be considered as intrinsic to the material and  
 232 slightly deteriorated by the microcracks appearing in the pellets during physi-  
 233 cal properties measurements. The submicron particle size distribution obtained  
 234 after magnesio-reduction corresponds well to that reported by Benyahia *et al.*  
 235 on mesostructured  $ZT = 1.4$  In<sub>0.25</sub>Co<sub>4</sub>Sb<sub>12</sub>. Unfortunately, the grain growth in-  
 236 duced during sintering cancels this microstructural feature and both thermal  
 237 conductivity and figure-of-merit are much closer from those obtained by fusion-  
 238 solidification-long term annealing [2, 18] or most recently by scanning laser  
 239 melting for higher In-content [41]. Nevertheless, our  $ZT$  value is most of the  
 240 time higher than those reported after solid state diffusion [39, 42, 43] or HPHT  
 241 technique [44]. Improving the SPS step to limit the grain growth, stabilizing  
 242 In<sub>0.22</sub>Co<sub>4</sub>Sb<sub>12</sub>/InSb nanocomposites or trying to form multifilled skutterudites  
 243 by magnesiothermy are the perspectives of this work.

## 244 **4. Conclusions**

245 The investigation of the reaction mechanism for the magnesio-reduction syn-  
 246 thesis of In-filled skutterudite from Sb<sub>2</sub>O<sub>4</sub> and In-doped Co<sub>3</sub>O<sub>4</sub> evidenced a  
 247 complex scenario involving intermediate species: CoO, Sb<sub>2</sub>O<sub>3</sub>, CoSb<sub>2</sub>O<sub>6</sub> and  
 248 CoSb<sub>2</sub>O<sub>4</sub>. The formation of CoSb<sub>3</sub> precedes the insertion of In-rattler in the  
 249 cage. After spark plasma sintering, the resulting material is single phase skut-  
 250 terudite with composition close to In<sub>0.22</sub>Co<sub>4</sub>Sb<sub>12</sub> which corresponds to the In-  
 251 richest composition which could be synthesized by this technique in these con-  
 252 ditions. A  $ZT_{max}$  of 0.95 is measured at 750 K due to limited  $PF$  resulting from  
 253 elevated  $\rho$  caused by microcracks appearing in the pellets. In addition to im-

portant energy and time saving, the relatively mild reaction conditions used in this process prevent high Mg vapors pressure inside the reactor thus avoiding the formation of deleterious Mg-containing side-products which often limits the up-scaling perspectives of magnesio-reduction processes. Finally, the knowledge gained on the reaction mechanism will be a precious help for the development of optimized reaction conditions (multi-step heat treatment, mixed oxide precursors) enabling the insertion of other filler atoms (*e.g.* Ba, rare earths elements) whose respective oxides are often too stable to be reduced by Mg in the present reaction conditions.

## Acknowledgements

Loic Joanny and Francis Gouttefangeas are acknowledged for SEM images and EDS analyses performed on the CMEBA platform belonging to the ScanMAT unit (UMS 2001, University of Rennes 1) which received a financial support from the European Union (CPER-FEDER 2007-2014).

## Declaration of interest

The authors declare no conflict of interest.

## References

- [1] G. Rogl, P. Rogl, Skutterudites, a most promising group of thermoelectric materials, *Curr. Opin. Green Sustainable Chem.* 4 (2017) 50–57.
- [2] J. Leszczynski, V. D. Ros, B. Lenoir, A. Dauscher, C. Candolfi, P. Masschelein, J. Hejtmanek, K. Kutorasinski, J. Tobola, R. I. Smith, C. Stiewe, E. Müller, Electronic band structure, magnetic, transport and thermodynamic properties of In-filled skutterudites  $\text{In}_x\text{Co}_4\text{Sb}_{12}$ , *J. Phys. D: Appl. Phys.* 46 (2013) 495106.



- 278 [3] X. Li, Q. Zhang, Y. Kang, C. Chen, L. Zhang, D. Yu, Y. Tian, B. Xu, High  
279 pressure synthesized Ca-filled  $\text{CoSb}_3$  skutterudites with enhanced thermo-  
280 electric properties, *J. Alloys Compd.* 677 (2016) 61–65.
- 281 [4] Y. Kang, F. Yu, C. Chen, Q. Zhang, H. Sun, L. Zhang, D. Yu, Y. Tian, B. Xu,  
282 High pressure synthesis and thermoelectric properties of Ba-filled  $\text{CoSb}_3$   
283 skutterudites, *J. Mater. Sci.: Mater. Electron.* 28 (2017) 8771–8776.
- 284 [5] G. S. Nolas, M. Kaeser, R. T. Littleton, T. M. Tritt, High figure of merit  
285 in partially filled ytterbium skutterudite materials, *Appl. Phys. Lett.* 77  
286 (2000) 1855.
- 287 [6] G. Rogl, A. Grytsiv, K. Yubuta, S. Puchegger, E. Bauer, C. Raju, R. Mallik,  
288 P. Rogl, In-doped multified n-type skutterudites with  $ZT = 1.8$ , *Acta*  
289 *Mater.* 95 (2015) 201–211.
- 290 [7] Y. Tang, Y. Qiu, L. Xi, X. Shi, W. Zhang, L. Chen, S.-M. Tseng, S. wen  
291 Chend, G. J. Snyder, Phase diagram of In-Co-Sb system and thermoelectric  
292 properties of In-containing skutterudites, *Energy Environ. Sci.* 7 (2014)  
293 812.
- 294 [8] A. Grytsiv, P. Rogl, H. Michor, E. Bauer, G. Giester,  $\text{In}_y\text{Co}_4\text{Sb}_{12}$  skutterudite:  
295 phase equilibria and crystal structure, *J. Electron. Mater.* 42 (2013) 2940–  
296 2952.
- 297 [9] E. Visnow, C. P. Heinrich, A. Schmitz, J. de Boor, P. Leidich, B. Klobes, R. P.  
298 Hermann, W. E. Müller, W. Tremel, On the true indium content of In-filled  
299 skutterudites, *Inorg. Chem.* 54 (2015) 7818–7827.
- 300 [10] R. C. Mallik, J. Y. Jung, S. C. Ur, I. H. Kim, Thermoelectric properties of  
301  $\text{In}_x\text{Co}_4\text{Sb}_{12}$  skutterudites, *Met. Mater. Int.* 14 (2008) 223.

- [11] M. Benyahia, V. Ohorodniichuk, E. Leroy, A. Dauscher, B. Lenoir, E. Alleno, High thermoelectric figure of merit in mesostructured  $\text{In}_{0.25}\text{Co}_4\text{Sb}_{12}$  n-type skutterudite, *J. Alloys Compd.* 735 (2018) 1096–1104.
- [12] J. Eilertsen, S. Rouvimov, M. Subramanian, Rattler-seeded InSb nanoinclusions from metastable indium-filled  $\text{In}_{0.1}\text{Co}_4\text{Sb}_{12}$  skutterudites for high-performance thermoelectrics, *Acta Mater.* 60 (2012) 2178–2185.
- [13] G. Li, K. Kurosaki, Y. Ohishi, H. Muta, S. Yamanaka, Thermoelectric properties of Indium-added skutterudites  $\text{In}_x\text{Co}_4\text{Sb}_{12}$ , *J. Electron. Mater.* 42 (2013) 1463.
- [14] H. Li, X. Su, X. Tang, Q. Zhang, C. Uher, G. J. Snyder, U. Aydemir, Grain boundary engineering with nano-scale InSb producing high performance  $\text{In}_x\text{Ce}_y\text{Co}_4\text{Sb}_{12+z}$  skutterudite thermoelectrics, *J. Materiomics* 3 (2017) 273–279.
- [15] C. Chubilleau, B. Lenoir, C. Candolfi, P. Masschelein, A. Dauscher, E. Guilmeau, C. Godart, Thermoelectric properties of  $\text{In}_{0.2}\text{Co}_4\text{Sb}_{12}$  skutterudites with embedded PbTe or ZnO nanoparticles, *J. Alloys Compd.* 589 (2014) 513–523.
- [16] Y. Du, K. Cai, S. Chen, Z. Qin, S. Shen, Investigation on Indium-Filled Skutterudite Materials Prepared by Combining Hydrothermal Synthesis and Hot Pressing, *J. Electron. Mater.*, year =.
- [17] A. Gharleghi, P.-C. Hung, F.-H. Lin, C.-J. Liu, Enhanced ZT of  $\text{In}_x\text{Co}_4\text{Sb}_{12}$ -InSb nanocomposites fabricated by hydrothermal synthesis combined with solid-vapor reaction: a signature of phonon-glass and electron-crystal materials, *ACS Appl. Mater. Interfaces* 8 (2016) 35123–35131.
- [18] S. Lee, K. H. Lee, Y.-M. Kim, H. S. Kim, G. J. Snyder, S. Baik, S. W. Kim,

- 327 Simple and efficient synthesis of nanograin structured single phase filled  
328 skutterudite for high thermoelectric performance, *Acta Mater.* 142 (2018)  
329 8–17.
- 330 [19] M. S. Toprak, C. Stiewe, D. Platzek, S. Williams, L. Bertini, E. Müller,  
331 C. Gatti, Y. Zang, M. Rowe, M. Muhammed, The impact of nanostruc-  
332 turing on the thermal conductivity of thermoelectric CoSb<sub>3</sub>, *Adv. Funct.*  
333 *Mater.* 14 (2004) 1189–1196.
- 334 [20] S. Le Tonquesse, E. Alleno, V. Demange, V. Dorcet, L. Joanny, C. Prestipino,  
335 O. Rouleau, M. Pasturel, Innovative one-step synthesis of mesostructured  
336 CoSb<sub>3</sub>-based skutterudites by magnesio-reduction, *J. Alloys Compd.* 796  
337 (2019) 176–184.
- 338 [21] S. Le Tonquesse, V. Dorcet, L. Joanny, V. Demange, C. Prestipino, Q. Guo,  
339 D. Berthebaud, T. Mori, M. Pasturel, Mesostructure - thermoelectric prop-  
340 erties relationships in V<sub>x</sub>Mn<sub>1-x</sub>Si<sub>1.74</sub> (x = 0, 0.04) higher manganese  
341 silicides prepared by magnesiothermy, *J. Alloys Compd.* in press (2020)  
342 doi:10.1016/j.jallcom.2019.152577.
- 343 [22] W. Kroll, Verformbares Titan und Zirkon, *Z. Anorg. Allg. Chem.* 234  
344 (1937) 42–50.
- 345 [23] F. H. Spedding, H. A. Wilhelm, W. H. Keller, Production of Uranium, U.S.  
346 Patent no. 2830894.
- 347 [24] E. Antolini, M. Ferretti, Synthesis and Thermal Stability of LiCoO<sub>2</sub>, *J. Solid*  
348 *State Chem.* 117 (1995) 1–7.
- 349 [25] L. Ma, C. Y. Seo, X. Chen, K. Sun, J. W. Schwank, Indium-doped Co<sub>3</sub>O<sub>4</sub>  
350 nanorods for catalytic oxidation of CO and C<sub>3</sub>H<sub>6</sub> towards diesel exhaust,  
351 *Appl. Catal. B-Environ.* 222 (2018) 44–58.

- 352 [26] J. Rodriguez-Carvajal, Recent advances in magnetic-structure determina-  
353 tion by neutron powder diffraction, *Physica B* 192 (1993) 55–69.
- 354 [27] O. Rouleau, E. Alleno, Measurement system of the Seebeck coefficient or of  
355 the electrical resistivity at high temperature, *Rev. Sci. Instrum.* 84 (2013)  
356 105103.
- 357 [28] H. Toraya, Estimation of statistical uncertainties in quantitative phase  
358 analysis using the Rietveld method and the whole-powder-pattern decom-  
359 position method, *J. Appl. Cryst.* 33 (2000) 1324–1328.
- 360 [29] O. Knacke, O. Kubaschewski, K. Hesselmann, *Thermo-chemical Properties*  
361 *of Inorganic Substances* (1991) Springer Ed.
- 362 [30] B. P. de Laune, C. Greaves, Structural and magnetic characterisation of  
363  $\text{CoSb}_2\text{O}_4$  and the substitution of  $\text{Pb}^{2+}$  for  $\text{Sb}^{3+}$ , *J. Solid State Chem.* 187  
364 (2012) 225–230.
- 365 [31] D. Larcher, A. S. Prakash, L. Laffont, M. Womes, J. C. Jumas, J. Olivier-  
366 Fourcade, M. S. Hedge, J.-M. Tarascon, Reactivity of antimony oxides and  
367  $\text{MSb}_2\text{O}_6$  ( $\text{M} = \text{Cu}, \text{Ni}, \text{Co}$ ) trirutile-type phases with metallic lithium, *J.*  
368 *Electrochem. Soc.* 153 (2006) A1778–A1787.
- 369 [32] J. N. Reimers, J. E. Greedan, C. V. Stager, R. Kremer, Crystal structure  
370 and magnetism in  $\text{CoSb}_2\text{O}_4$  and  $\text{CoTa}_2\text{O}_6$ , *J. Solid State Chem.* 83 (1989)  
371 20–30.
- 372 [33] T. He, J. Chen, H. D. Rosenfeld, M. A. Subramanian, Thermoelectric prop-  
373 erties of indium-filled skutterudites, *Chem. Mater.* 18 (2006) 759–762.
- 374 [34] S.-J. L. Kang, *Sintering: densification, grain growth and microstructure*  
375 (2004) Elsevier Ed.

- [35] J. Eilertsen, Y. Surace, S. Balog, L. Sagarna, G. Rogl, J. Horky, M. Trottman, P. Rogl, M. A. Subramanian, A. Weidenkaff, From occupied voids to nanoprecipitates: synthesis of skutterudite nanocomposites in situ, *Z. Anorg. Allg. Chem.* 641 (2015) 1495–1502.
- [36] J.-Y. Jung, K.-H. Park, S.-C. Ur, I.-H. Kim, Thermoelectric and transport properties of In-filled  $\text{CoSb}_3$  skutterudites, *Mater. Sci. Forum* 658.
- [37] R. C. Mallik, C. Stiewe, G. Karpinski, R. Hassdorf, E. Müller, Thermoelectric properties of  $\text{Co}_4\text{Sb}_{12}$  skutterudite materials with partial In filling and excess In additions, *J. Electron. Mater.* 38 (2009) 1337–1343.
- [38] A. Sesselmann, T. Dasgupta, K. Kelm, E. Müller, S. Perlt, S. Zastrow, Transport properties and microstructure of indium-added cobalt-antimony-based skutterudites, *J. Mater. Res.* 26 (2011) 1820–1826.
- [39] J. Peng, X. Liu, L. Fu, W. Xu, Q. Liu, J. Yang, Synthesis and thermoelectric properties of  $\text{In}_{0.2+x}\text{Co}_4\text{Sb}_{12+x}$  composite, *J. Alloys Compd.* 521 (2012) 141–145.
- [40] V. V. Khovaylo, T. A. Korolkov, A. I. Voronin, M. V. Gorshenko, A. T. Burkov, Rapid preparation of  $\text{In}_x\text{Co}_4\text{Sb}_{12}$  with a record-breaking  $ZT=1.5$ : the role of the In overfilling fraction limit and Sb overstoichiometry, *J. Mater. Chem. A* 5 (2017) 3541–3546.
- [41] F. Chen, R. Liu, Z. Yao, Y. Xing, S. Bai, L. Chen, Scanning laser melting for rapid and massive fabrication of filled skutterudites with high thermoelectric performance, *J. Mater. Chem. A* 6 (2018) 6772–6779.
- [42] K. Biswas, M. A. Subramanian, M. S. Good, K. C. Roberts, T. J. Hendricks, Thermal cycling effects on the thermoelectric properties of *n*-type In,Ce-based skutterudite compounds, *J. Electron Mater.* 41 (2012) 1615–1621.

- 401 [43] A. Sesselmann, B. Klobes, T. Dasgupta, O. Gourdon, R. Hermann,  
402 E. Müller, Neutron diffraction and thermoelectric properties of in-  
403 dium filled  $\text{In}_x\text{Co}_4\text{Sb}_{12}$  ( $x = 0.05, 0.2$ ) and indium cerium filled  
404  $\text{Ce}_{0.05}\text{In}_{0.1}\text{Co}_4\text{Sb}_{12}$ , Phys. Status Sol. A 213 (2016) 766–773.
- 405 [44] L. Deng, L. B. Wang, J. M. Qin, T. Zheng, Effects of indium-filling and  
406 synthesis pressure on the thermoelectric properties of  $\text{CoSb}_3$ , Mod. Phys.  
407 Lett. B 28 (2014) 1450118.